Quantum Cosmology and the Role of Consciousness

Arthur E. Pletcher*

ABSTRACT

Neuroscience has theorized the "two minds" model of the human brain from research on post-surgery "dual consciousness" of split-brain patients (Vitiellon, 2003). This article attempts to explain the functioning role of oppositional consciousness dynamics, and how it interacts with quantum mechanics. This article proposes that consciousness is an interactive process of polarizing an observed source of higher dimensional $\mathbb{R}^5$ space onto a (cognitively modeled) collapsed $\mathbb{R}^4$ space. The dynamics of this process involve escalating (reinforcement loop) interaction within the dual and opposing mind of a single observer. This polarized (collapsed space) results in a lower dimensional, yet higher codomain range, and resulting increased entropy. Analogies are drawn between familiar classic space information exchanges (such as tribal disputes) and decoherence in quantum information theory. An intuitive and familiar example of escalating tribal dispute dynamics is constructed and formulated. The subsequent entropic effects of information exchange are then calculated as transitioning from Gaussian to power-law distribution. The resulting topology, inscribed wave patterns, superposition, collapse, constructive and destructive interference, and discrete energy are alternatively presented. This model is then generally framed within the full scope of cosmology, from Planck scale to Macro-scale, to explain the effects of accelerating expansion and galaxy rotation curves. Relativity effects are also calculated. Speculation is avoided with mathematical evidence and patterns.

DOI Number: 10.14704/nq.2019.17.01.1934 **NeuroQuantology 2019; 17(01):104-111**

Introduction

This article presents analogies between familiar classic space information exchange (such as tribal disputes) and decoherence in quantum information theory (Collapse of the wave function in quantum mechanics) (Gunhann, 2014), and proposes a natural connection between the two scales, beginning with the ubiquitous presence of distortion. In familiar classic space, the interaction between information and its local environment typically results in some degree of distortion. This principle is demonstrated in the game of "Chinese Whispers", where recursive communication results in a fundamental distorted shift of information from its original source. Often, such information exchange takes the form of a reinforcement loops, where distortions and responses co-escalate exponentially. Reinforcement loop interaction seems to be ubiquitous throughout nature, and on every scale. It seems reasonable to assume that escalating reinforcement loop interaction is fundamental to the structure of information, in general.

Modeling Distortion as Partial Gnomonic Mapping

Let open sets p1 and p2 be partial nonconformal gnomic mappings of sphere S onto two tangent planes at different (non-antipodal) surface parameters, with a mutual minute difference in orientation of $\frac{d\theta}{dt}$. See Fig. 1.

$$S \in \mathbb{R}^3_{def} = (x, y, z) \in \mathbb{R}^2 : \left\| x^2 + y^2 + z^2 = r \right\| \quad (1)$$

$$F : S \to /(p_1, p_2) \quad (2)$$

Note the discrepancy between these two non-antipodal projected coordinate points within their respective open sets: Each disk shares a set of

Corresponding author: Arthur E. Pletcher
Address: International Society for Philosophical Enquiry, Winona, Minnesota, USA
e-mail ✉ artpletcher@ultrahighiq.org
Relevant conflicts of interest/financial disclosures: The authors declare that the research was conducted in the absence of any commercial or financial relationships that could be construed as a potential conflict of interest.
Received: 18 December 2018; **Accepted:** 14 January 2019

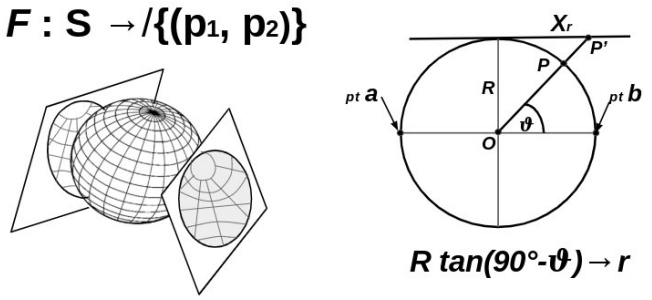


Figure 1. Mappings of sphere S onto two tangent planes.

common points $(p_1 \subset S)$ and $(p_2 \subset S)$, as well as a set of mutually separated points $(p_1 \cap p_2)$ such that:

$$(p_1 \cap p_2) \geq 1 \text{ and } < p_1 \cup p_2 \quad (3)$$

$$p_1 \setminus p_2 \geq 1 \text{ and } < p_1 \cup p_2 \quad (4)$$

$$(p_1 \cap p_2)^c > 0 \quad (5)$$

Meridian's (orthodromes) are projected as lateral straight lines. Parallels are transversely scaled per (Coxetern, 1969):

$$x_r = R \tan(\frac{\pi}{2} - \theta) \quad (6)$$

An obvious, yet significant derivation of equation 6 and Fig. 1 is:

Theorem 2.1 *If open set p_2 is a nonconformal gnomonic projection of sphere S at a tangent surface plane, then from the reference frame (r.f.) of an $\mathbb{R}^2$ observer at plane P, projected antipodal points a and b which are normal to plane P appear to be infinitely separated at the bipolar horizon (as the transverse scale is asymptotic to R). However, from the (r.f.) of an $\mathbb{R}^3$observer on sphere S, antipodal points a and b are connected in higher dimensional topology, per radius R:*

$$R = \frac{x_r}{\tan(\frac{\pi}{2} - \theta)} \quad (7)$$

Tribal Conflict Reinforcement Loops as Decoherence

Minute discrepancies between elements engaged in reinforcement loops result in exponential growth or decay. Such dynamic information exchange between two rational agents is generalized in the following example: (See Fig. 2 and formal definitions).

Formal Definitions for Fig. 2

$$a, b \in C$$

F : a → /b = partial gnomonic mapping of element a onto element b

B_i = Initial condition discrepancy bias of a, b

f_n = iteration (n)

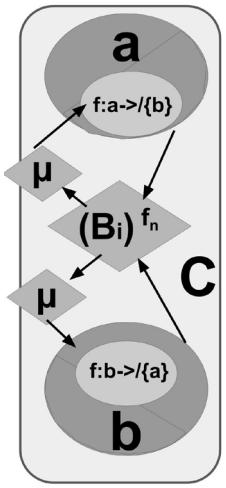


Figure 2. Tribal Conflict Reinforcement Loops.

SV = Self validation, or meta – validation

R_n = Dimensional space (n)

μ = Measures

F : a → /b is used to designate a partial gnomonic mapping of element (a) onto element (b), and comparing the image range with the codomain. The intention is to capture distortions from exchanges between biased states.

Note that recursive iterations result in reduced degrees of freedom (d.o.f.) and increased entropy.

Two tribes, *a* and *b*, are engaged in some dispute. Both tribes seek a state of homeostasis with the greater external set (*c*). However, their innate mutual discrepancy ΔB_i defies resolution, as they both assume themselves to be center aligned with (*c*), and their counterpart to be shifted from center. Let the initial condition $= \Delta B_i$ (initial mutual discrepancy). Assume the complimentary union of $(a \cap b)^c > 0$ (See Fig. 3). The following sequence emerges (see Fig. 4):

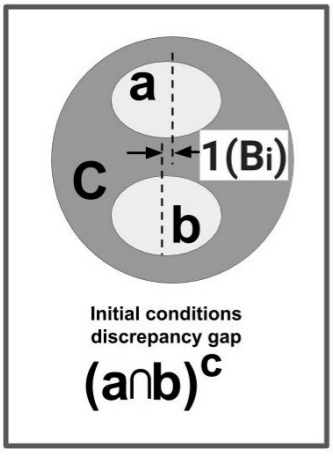


Figure 3. Initial condition of elements a and b, within set c.

f^n	a μ b (Bi)	F: a→/{b} (Bi)	Δ (Bi)	b μ a (Bi)	F: b→/{a} (Bi)	Δ (Bi)
1	+1	-1	2	-2	+2	4
2	+4	-4	8	-8	+8	16
3	+16	-16	32	-32	+32	64
4	+64	-64	128	-128	+128	256

Figure 4. Tribal dispute reinforcement loops as decoherence.

Iteration f^1,

1. $a \mu b = +1(\overrightarrow{B_i})$ (*a* assumes to be at center of set *c*, and measures *b* to be shifted by $+1(\Delta B_i)$)
2. $F: a \rightarrow /b$ (a responds to b with countermeasures of equal magnitude $-1(\overrightarrow{\Delta B_i})$
3. $b \mu a = -2(\overrightarrow{\Delta B_i})$ (*b* assumes to be at center of set *c*, and measures *a* to be shifted by $-2(\overrightarrow{\Delta B_i})$)
4. $F: b \rightarrow /a$ (*b* responds to *a* with countermeasures of equal magnitude $+2(\overrightarrow{\Delta B_i})$)
5. Mutually, the assumptions and assessments of both *a* and *b* are validated (self-validated).

Iteration f^2,

1. $a \mu b = +4(\overrightarrow{\Delta B_i})$ (*a* assumes to be at center of set *c*, and measures *b* to be shifted by $+4(\overrightarrow{\Delta B_i})$)
2. $F: a \rightarrow /b$ (*a* responds to *b* with countermeasures of equal magnitude $-4(\overrightarrow{B_i})$
3. $b \mu a = -8(\overrightarrow{B_i})$ (*b* assumes to be at center of set *c*, and measures *a* to be shifted by $-8(\overrightarrow{B_i})$)
4. $F: b \rightarrow /a$ (*b* responds to *a* with countermeasures of equal magnitude $+8(\overrightarrow{\Delta B_i})$)
5. Mutually, the assumptions and assessments of both *a* and *b* are validated (self-validated).

[...]

For this generalized reinforcement loop model, the exponential growth rate *g* at any iteration f^n is simply:

$$4^n + (B_i - 1) \quad (8)$$

Entropic Effects of Information Exchange Within Reinforcement Loops

Equation 8 describes the exponential development of a generalized information exchange within a reinforcement loop. The inevitable result of such recursive exchanges is a power law distribution, with associated increased entropy. (See Fig. 5).

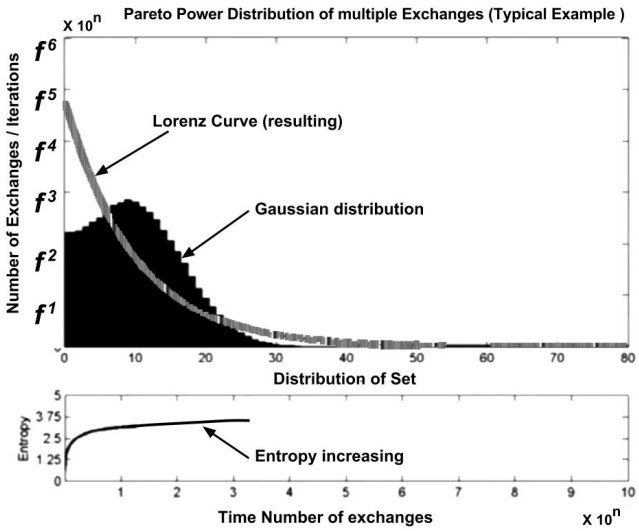


Figure 5. Typical Pareto distribution from Gaussian, after multiple exchanges

Power law of recursive exchanges

$$p(x) = Cx^{\alpha} = \frac{C}{x_{\alpha}}, for\, x \geq x_{min}$$

Normalization for $(\alpha > 1)$

$$1 = \int_{x_{min}}^{\infty} p(x)\,dx = C \int_{x_{min}}^{\infty} \frac{dx}{x^{\alpha}} = \frac{C}{\alpha - 1} x_{min}^{-\alpha+1}$$

$$C = (\alpha - 1) x_{min}^{-\alpha+1}$$

Power law probability function (PDF)

$$p(x) = \frac{\alpha - 1}{x_{min}} \left(\frac{x}{x_{min}} \right)^{\alpha}$$

(Newmann, 2005) Per the Entropy-Power Inequality:

$$\exp(2h(X+Y)) \geq \exp(2h(X)) + \exp(2h(Y)) \quad (9)$$

(Shannonn, 1963) Where X and *Y* are independent real-valued random variables and *h(X)* is the differential entropy of the PDF.

Visual Intuition of $\mathbb{R}^2$ Topology "Collapsed" Onto an $\mathbb{R}^1$ Plane

Let's compare the initial state vs the resulting escalated state, in the tribal conflict example. The initial state was isotropic and only slightly out of equilibrium. It's interaction can be described with an $\mathbb{R}^2$ matrix of range magnitude ΔB_i. However, the

interaction of the resulting polarized state became limited to a $\mathbb{R}^1$ matrix with a much higher range magnitude per equation 8. It seems reasonable to consider the latter state as collapsed, with a mutual trade-off between range magnitude and symmetry.

The following topology is proposed, for intuition: Consider a set whose five elements are arranged in the lower half of a circle, with a magnitude range of *2r.* it's $\mathbb{R}^2$ matrix representation would be (in Cartesian coordinates):

$$\begin{bmatrix} 1r & 0r \\ \frac{\sqrt{2}}{2}r & -\frac{\sqrt{2}}{2}r \\ 0r & -1r \\ -\frac{\sqrt{2}}{2}r & -\frac{\sqrt{2}}{2}r \\ -1r & 0r \end{bmatrix}$$

Now, let these five elements become polarized in the direction of the *X* coordinate, such that r approaches infinity at an exponential rate. See Fig. 6. This morphing of $\mathbb{R}^2$ onto an $\mathbb{R}^1$ space can be described as a collapse.

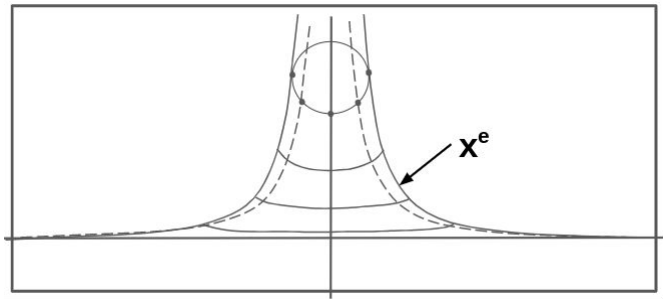


Figure 6. $\mathbb{R}^2$ circular arrangement of elements collapsed onto $\mathbb{R}^1$ space

$$\begin{bmatrix} r\pi \\ \frac{r\pi}{2} \\ 0r \\ -\frac{r\pi}{2} \\ -r\pi \end{bmatrix} \lim_{r\to\infty}$$

Another simple corollary to theorem 2.1 is worth noting:

Corollary 5.0.1 *Polarization skews the space between elements, such that transverse scales increase per equation 6. From the perspective of the polarized (collapsed) state, space is expanding outward from the center and subsequently motion* $\underline{\vec{v}}$ *appears accelerated over distance d.*

A Higher Dimensional R^3 Space Appears as Superimposed

Consider the perspective of an observer on an $\mathbb{R}^2$ plane. How would a moving particle, in a rotating higher dimensional $\mathbb{R}^3$ space appear from his lower dimensional reference frame (r.f.) Fig. 7 shows how such a rotating moving particle inscribes a wave pattern (standing wave, in position (*Y*) as a function of (x), per equation:

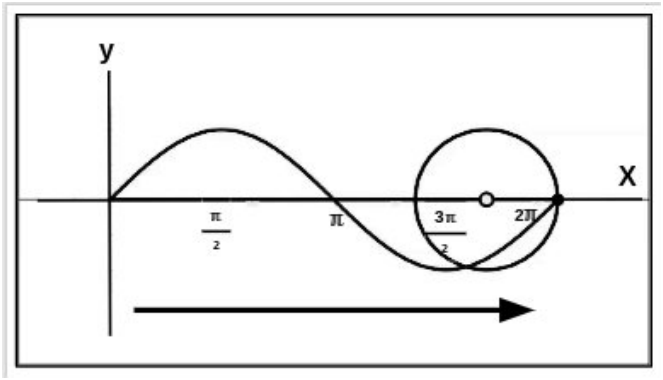


Figure 7. Rotating moving particle inscribes a wave pattern

$$y(x) = A\sin(\omega x + \theta) \quad (10)$$

Superposition and Discrete Energy from the $\mathbb{R}^n$ r.f

As dimension *z* is hidden from the $\mathbb{R}^2$ *x, y* plane, it's fair to describe the energy along dimension *z* as being superimposed (multiple states in a single *x, y* coordinate) from the $\mathbb{R}^2$ r.f. As well, discrete gaps naturally occur along the *x, y* intercept, as the higher dimensional particle moves in and out (along *z*) of the *x, y* plane (keeping in mind that $\mathbb{R}^2$'s entire existence is limited to the *x,y* plane.

Extending Collapse Topology to Classic Space-time

We can Extend the same $\mathbb{R}^2$ visual intuition of Fig. 6 to an $\mathbb{R}^5$ "hyper-space and time" geometry of matrix $(x_1, x_2, x_3, x_4, x_5)$ and thus collapsing onto an $\mathbb{R}^4$ classic spacetime matrix of (x_1, x_2, x_3, x_4). Fig. 8 illustrates a rough conceptual intuition of such a collapse in higher dimensions. A corollary to Theorem 2.1 and 2nd corollary to 5.0.1 would then be:

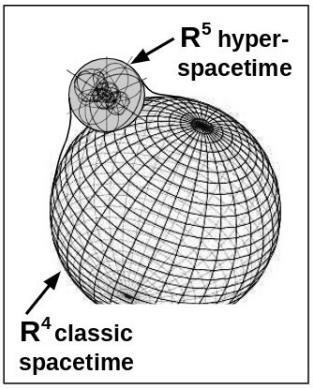


Figure 8. $\mathbb{R}^5$ "hyper-space and time" geometry collapsing onto an $\mathbb{R}^4$ classic-spacetime

Corollary 7.0.1 *Conscious interaction of Planck scales from an observer at classic space are functionally a mapping of an $\mathbb{R}^5$ hyperspace and time topology onto an R^4 classic spacetime collapsed state. This collapsed space is polarized, of a lower dimension, and result in a higher range, along with an increase of entropy.*

From the reference frame of $\mathbb{R}^4$ classic spacetime, the $\mathbb{R}^5$ hyper-orbit appears as a superimposition of momentum, position and time. At the point when the observer interacts in an escalating feedback loop, the polarized collapsed $\mathbb{R}^4$ state emerges.

Extending the Inscribed Wave (of section 6) to R^4 Classic Spacetime

From the R.F. of an observer in $\mathbb{R}^4$ classic spacetime, a moving particle in $\mathbb{R}^5$ hyperspace (and time) inscribes a 3D transverse wave in position *x, y, z* and time *t*, per equation:

$$y(x,y,t) = A\sin(kx-\omega t) + B\cos(kx-\omega t) \quad (11)$$

Note, the fourth spatial dimension (x_4) of the $\mathbb{R}^5$ hypersphere is hidden from the observer in $\mathbb{R}^4$ classic space, and thus appears to be in superposition.

In the absence of an external force, it's total energy (potential and non-relativistic kinetic energy) can be expressed as (Bransdenn and Joachainn, 1983):

$$E = \frac{k^2\hbar^2}{2m} + U \quad (12)$$

See Fig. 9.

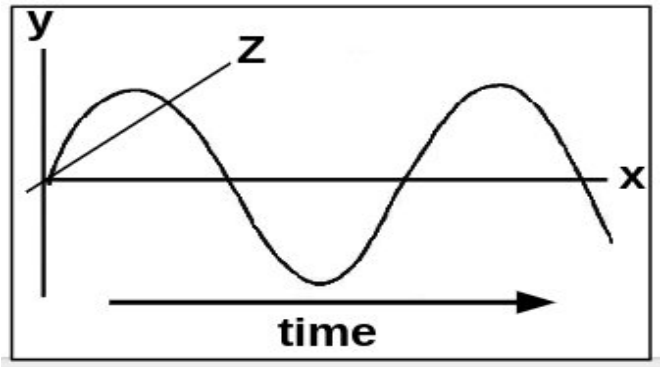


Figure 9. From $\mathbb{R}^4$ R.F., an $\mathbb{R}^5$ hyper-space and time orbit inscribes a 3D traveling wave, which appears to be in superposition

This system can be described by the 3-D Schrodinger equation (Brandtn and Dahmenn, 2000):

$$\frac{-\hbar^2}{2m}\left[\frac{\partial^2\psi}{\partial x^2}+\frac{\partial^2\psi}{\partial y^2}+\frac{\partial^2\psi}{\partial z^2}\right]+U(x,y,z)\psi(x,y,z) = E\psi(x,y,z) \quad (13)$$

However in this alternative model, wave-particle duality is determined by an active process of consciousness. Thus, equation 11 describes the state before conscious interaction, and equation 12 describes the collapsed post conscious interaction state.

Also by extension, discrete (quantum) energy is the natural result of an $\mathbb{R}^5$ particle moving in and outside of the realm of observations within $\mathbb{R}^4$ classic space and time. As well, values of energy, position and charge in the $\mathbb{R}^5$ fourth spatial dimension appears to be in superposition (multiple values in a single coordinate) to the r.f. of observers residing in $\mathbb{R}^4$ classic space and time.

Mathematical Evidence of This Model in Macrospace

This model of collapsing topology (entropic polarization, expanded range and dimensional reduction) can be extended onto macrospace, as well. It is particularly suited to explain the accelerating effects of macrospace alternatively as projected skewed topology.

Redshifting as Skewed Projected Topology

In Fig. 10, transverse parallels are projected asymptotic to the horizon. Framed within this model, electromagnetic wavelengths λ which emanate from the $\mathbb{R}^5$ hypersphere, along arc length *a* are constant. However, wavelength λx is projected (and skewed) along the *x* axis and redshifted as a result, similar to the redshifting equation (Taylorn and Wheeler, 1992):

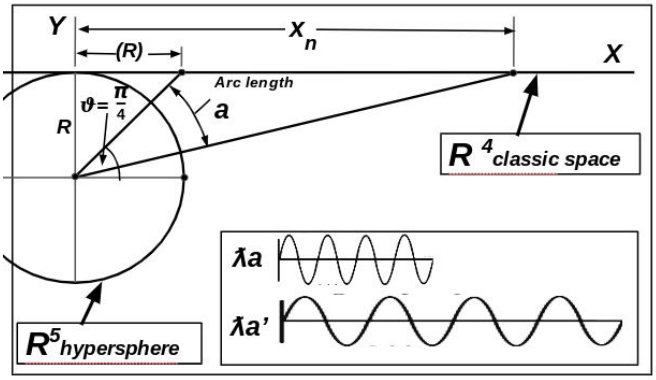


Figure 10. $\mathbb{R}^5$ Hypersphere projected onto an $\mathbb{R}^4$ classic space, and extended into macrospace

$$z = \frac{\lambda_{obs} - \lambda_{rest}}{\lambda_{rest}} \quad (14)$$

In this alternative model, arclength *a* is substituted for λ_{rest} and projected length *x* is substituted for λ_{obs} as (Refer to Fig. 10):

$$z = \frac{x-a}{a} \quad (15)$$

Where $a = 2R\pi * \frac{\left(\frac{\pi}{2}-\theta\right)}{2\pi} = R\left(\frac{\pi}{2}-\theta\right)$ (16)

and $x = R\tan\left(\frac{\pi}{2}-\theta\right)$, similar to equation 6 thus, (17)

$$z = \frac{R\tan\left(\frac{\pi}{2}-\theta\right) - R\left(\frac{\pi}{2}-\theta\right)}{R\left(\frac{\pi}{2}-\theta\right)} = \quad (18)$$

$$z = \frac{R\left(\tan\left(\frac{\pi}{2}-\theta\right) - \left(\frac{\pi}{2}-\theta\right)\right)}{R\left(\frac{\pi}{2}-\theta\right)} = \quad (19)$$

$$z = \frac{\tan\left(\frac{\pi}{2}-\theta\right) - \left(\frac{\pi}{2}-\theta\right)}{\left(\frac{\pi}{2}-\theta\right)} \quad (20)$$

Calculating Hypersphere Radius R

The radius R of the source $\mathbb{R}^5$ hypersphere can be deduced from this diverging series of redshift values. Although R can be derived from equation 7 in the $\mathbb{R}^5$ r.f., the $\mathbb{R}^4$ r.f. (Where humans reside) is limited to only projected points. Regardless of this limitation, we know from equation 7 that (R) in the x direction must be equal to radius R when the tan of θ is equal to 1, or when $\theta = \frac{\pi}{4}. z = \frac{\tan\frac{\pi}{4} - \frac{\pi}{4}}{\frac{\pi}{4}} \Rightarrow$ (21)

$$z = \frac{1-\frac{\pi}{4}}{\frac{\pi}{4}} \Rightarrow \quad (22)$$

$$z = 0.273 \quad (23)$$

Using the approximate distance formula for R:

$$d \approx \frac{zc}{H_0} \quad (24)$$

At current H0 value of: 73.8km/sec/Mpc

$$R \approx \frac{0.273 * 299792\, km/sec}{73.8\, km/sec/Mpc} \Rightarrow \quad (25)$$

Thus, the radius of the R5 hypersphere:

$$R \approx 1108.987\, Mpc \quad (26)$$

Velocity Appears to Increase Along Projected Length x

Referring to Fig. 10. Light-waves and energy density are constant along arclength a (along the $\mathbb{R}^5$ hypersphere). However from the r.f. of an observer on the projected length x, topology is skewed (elongated). Light-waves travel along x with an apparent increased velocity $\vec{v}'$ of:

$$\frac{\vec{v}'}{v} = \frac{x}{a} \quad (27)$$

Relativity Effects of Increased Velocity $\vec{v}$ Along Projected Skewed Length x

Per Special Relativity, time dilation occurs when an observer measures, from his r.f., the light clock of another r.f., which is in relative motion as being slower, per time dilation (Bornn, 1964):

$$t' = t\sqrt{\frac{1-V^2}{c^2}} \quad (28)$$

Thus, the logical contrapositive of this theorem is a time contraction:

Theorem 9.1 Time contraction Δt_n occurs when an observer measures, from his r.f., the light clock of another r.f., which is in relative motion as being faster. However, the contracting effects are due only to the skewed projection of information. (from equations 17, 18 and 27)

Δt_n *can be calculated as*:

$$\frac{\Delta t_n}{\Delta t} = \frac{x}{a} \Rightarrow$$

$$\frac{\Delta t_n}{\Delta t} = \frac{R\left(\frac{\pi}{2}-\theta\right)}{R\tan\left(\frac{\pi}{2}-\theta\right)} = \frac{\left(\frac{\pi}{2}-\theta\right)}{\tan\left(\frac{\pi}{2}-\theta\right)} \quad (30)$$

For example, at R =108,987 Mpc, and $\theta = \frac{\pi}{4}$:

$$\frac{\Delta t_n}{\Delta t} = \frac{\pi}{4} \quad (31)$$

Calculating z per Distance x

Now that R (The radius of the $\mathbb{R}^5$ hypersphere) has been established, values of z can be determined from any value of x. Note that x is the distance which humans measure galactic distance, although it is actually a skewed projection of arclength a (along

the $\mathbb{R}^5$ hypersphere). Thus, from values of distance modulus μ and radius R, theta is easily determined. Subsequently from theta, arc-length a is determined. Finally from equation 15, z is derived. However, luminosity is also affected along skewed distance x. Prior to deriving z from x, distance d from distance modulus μ must be adjusted. In this model μ becomes skewed (dimmer) as x increases Thus, a standard candle is closer than it appears by:

Using $d = 10^{\frac{u}{5}+1}$, then (32)

$$d' = \left(10^{\frac{u}{5}+1}\right)^{\frac{1}{k}} \quad (33)$$

$$= 10^{\frac{u}{5}+1\frac{1}{k}} \quad (34)$$

If d must be adjusted to d' along x, then it follows that R (the radius of the hypersphere) must also be adjusted proportionately to R':

$$R' = R^{\frac{1}{k}} \quad (35)$$

Setting k to = 1.786, (36)

$$R' = 50.783\,Mpc \quad (37)$$

Fig. 11 shows two graphs of extrapolated points at values of distance modulus μ vs z values The bottom graph is a log scale in the x-axis. **Note the familiar change in slope which is conventionally interpreted as "accelerating universal expansion".**

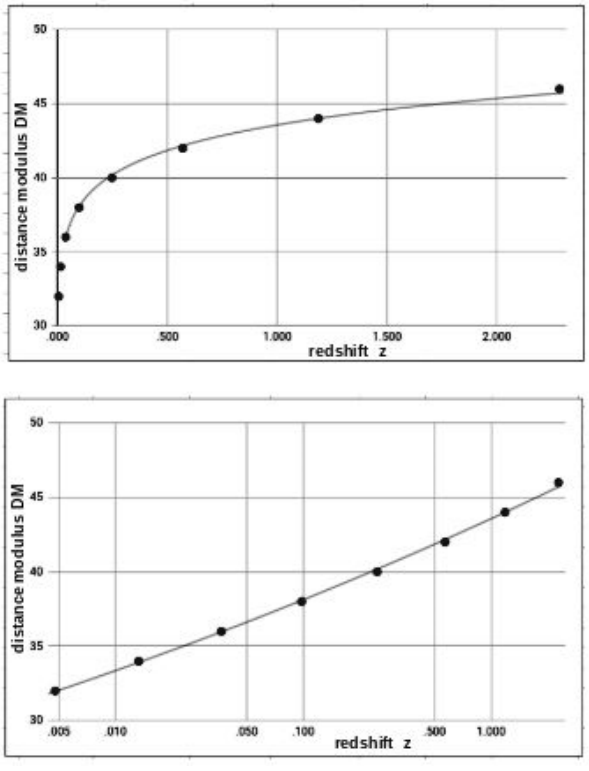


Figure 11. Scatter plots of distance modulus μ vs z

Energy Density Increases with Projected Length x

Corollary 10.0.1 *As velocity along skewed x appears to increase per equation 27, energy density ρ proportionally increases, due to increased velocities in particle kinetic and internal energies (compression, energy of nuclear binding, etc.). The observer at x = 0 measures volume at* x_n *[mpc] with increased energy density* ρ_n*, per equation:*

$$\frac{\Delta\rho_n}{\Delta\rho} = \frac{x}{a} \quad (38)$$

Galaxy Rotation Curve with Increased Density

The discrepancies between theoretical and observed galaxy rotation curves involve both density and velocity. Conventionally, the dependence of circular velocity v_{circ} on radial distance R assumes M, m and velocity to be fixed over large scales in Kepler's law, (Butikovn, 2014)

$$T^2 = \frac{4\pi^2 r^3}{GM} \Rightarrow T^2 \propto r^3$$

Moreover, gravitational lensing demonstrates the existence of a much greater Mass (density) than the sum of the stars within the galaxy. **However, this alternate model specifically addresses these two issues and provides an explanation**,

Corollary 10.0.2 *Velocity* $\vec{\underline{v}}$ *and density* ρ_n *are measured with increased magnitude per distance* x_n*. This directly extends to energy density within galaxies and the effects on rotational velocity, such that: As* x_n *increases, centripetal force is perfectly balanced by increases in* $\vec{\underline{v}}$ *and, subsequently,* ρ_n

$$\frac{v^2}{r} = \frac{G}{r^2}M = \frac{G}{r^2}\int \rho_n^{dt} \quad (39)$$

Note: total mass M inside the circle of the radius r can be obtained by doing integration of mass density in a volume

$M = \int \rho_n^{dt}$, $\rho = \rho_r$ *and* ρ_M (Dark components are excluded from this model, with the intent of presenting an alternative).

Conclusion

This article has presented an analogy between the polarization of information through conscious interaction, and quantum decoherence (Collapse of the wave function in quantum mechanics). Perhaps because polarization dynamics are so common and ubiquitous throughout nature, that they are easily overlooked as being functionally relevant, in a similar way that water is oblivious to a fish. However, information exchange is rarely linear,

rather dramatic exponential growth is typical. This underlying principle has been described in this article with the general example of escalating tribal disputes, but is also very common in politics and in all observable relationships between conscious rational agents. Equally analogous, are the resulting entropic effects between classic polarization dynamics and quantum decoherence. The presented model of an $\mathbb{R}^5$ hypersphere collapse onto an $\mathbb{R}^4$ classic space is precisely formulated. It has also been extended into macrospace, with a scatter plot closely fitting recent supernovae cosmology project data. If this model were to be proven correct, a fundamental unification would be established between all scales of information exchange and disciplines from Quantum Mechanics to Classic space and onto General Relativity. As well, a great many mysteries would be resolved, including superposition, wave function collapse, galaxy rotation curves, and universal accelerated expansion.

The model's mathematical simplicity and parsimonious concept provides some degree of support. However, one suggestion for empirical evidence would be through experimentation in the intermediate "mesoscopic" state. An $\mathbb{R}^n$ transition, similar to Fig. 6 might be proven by demonstrating the existence of both states simultaneously (a higher dimensional and isotropic state, coupled with a polarized lower dimensional state). The model, as described in this article, predicts an overlapping between the two scales such that measurable events (an electron excitement, etc) would interact simultaneously between both metrics. Fig. 13 illustrates how a single event occurring in materials, which are in a mesoscopic state, might be evident in two separate locations simultaneously. Proof would

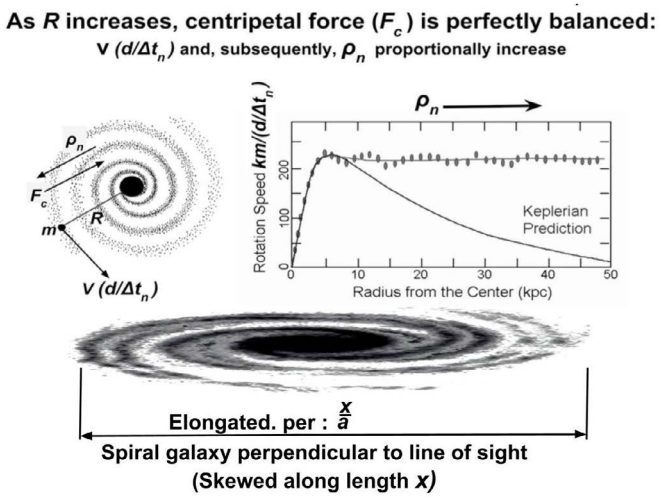


Figure 12. Galaxy Rotation Curve with Increased Density

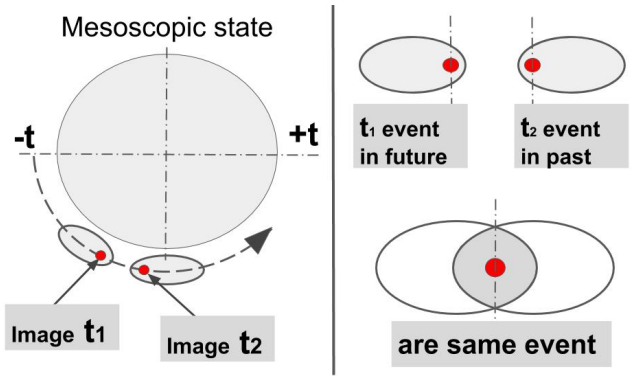


Figure 13. Two images at mesoscopic state represent the same single event at two points in time

need to be in the mathematical relationship between the two $\mathbb{R}^n$ metrics.

A Macrospace approach to finding evidence for this same model would be through correlating local group galaxies which have a negative z value (approaching instead of receding), with distance from Earth. This model predicts that these receding galaxies would also correlate with distance, per equation 20, such that the furthest galaxies would appear to approach with the fastest velocity. Such a high negative correlation would defy conventional theories.

References

Bornn M. Einstein's Theory of Relativity. Dover Publications, New York, 1964.

Brandtn S, and Dahmenn HD. The Picture Book of Quantum Mechanics. Springer-Verlag, New York, 2000.

Bransdenn BH, and Joachainn CF. Physics of Atoms and Molecules. Pearson, London, 1983.

Butikovn E. Motions of Celestial Bodies. IOP Publishing, Philadelphia, 2014.

Coxetern H. Introduction to Geometry (2). Wiley, Man hattan, 1969.

Gunhann AC. A toy model for memory: Memory can be represented by a quantum mechanical wave-function. SDU Journal of Science (e-journal) 2014; 9(1): 125-129.

Newmann M. Power laws, pareto distributions and zipf's law. Contemporary Physics 2005; 5(46): 323-351.

Shannonn C. A Mathematical Theory of Communication. University of Illinois Press, Champaign, 1963.

Taylorn E, and Wheeler JA. Spacetime Physics. WH Freeman and Company, New York, 1992.

Vitiellon G. Quantum dissipation and information: A route to consciousness modeling. NeuroQuantology 2003; 1(2): 266-279.